Journal of Solid State Chemistry 182 (2009) 1188–1192

Contents lists available at ScienceDirect

Journal of Solid State Chemistry

journal homepage: www.elsevier.com/locate/jssc

Structural properties of $Pb_3Mn_7O_{15}$ determined from high-resolution synchrotron powder diffraction

Julia C.E. Rasch [a,b,*], D.V. Sheptyakov [b], J. Schefer [b], L. Keller [b], M. Boehm [a], F. Gozzo [c], N.V. Volkov [d], K.A. Sablina [d], G.A. Petrakovskii [d], H. Grimmer [e], K. Conder [e], J.F. Löffler [f]

[a] Institut Laue-Langevin, 6 rue Jules Horowitz, BP 156, 38042 Grenoble Cedex 9, France
[b] Laboratory for Neutron Scattering, ETH Zurich and Paul Scherrer Institut, CH-5232 Villigen, PSI, Switzerland
[c] Swiss Light Source, Paul Scherrer Institut, CH-5232 Villigen, PSI, Switzerland
[d] L.V. Kirensky Institute of Physics, SB RAS, Krasnoyarsk 660036, Russia
[e] Laboratory for Developments and Methods, Paul Scherrer Institut, CH-5232 Villigen, PSI, Switzerland
[f] Laboratory of Metal Physics and Technology, Department of Materials, ETH Zurich, 8083 Zurich, Switzerland

ARTICLE INFO

Article history:
Received 12 November 2008
Received in revised form
27 January 2009
Accepted 1 February 2009
Available online 12 February 2009

PACS:
61.05.cp
75.47.Lx
61.66.−f

Keywords:
Manganites
Layered compounds
Powder X-ray diffraction

ABSTRACT

We report on the crystallographic structure of the layered compound $Pb_3Mn_7O_{15}$. Previous analysis based on laboratory X-ray data at room temperature gave contradictory results in terms of the description of the unit cell. Motivated by recent magnetic bulk measurements of this system [N.V. Volkov, K.A. Sablina, O.A. Bayukov, E.V. Eremin, G.A. Petrakovskii, D.A. Velikanov, A.D. Balaev, A.F. Bovina, P. Boni, E. Clementyev, J. Phys. Condens. Matter 20 (2008) 055217], we re-investigated the chemical structure with high-resolution synchrotron powder diffraction at temperatures between 15 and 295 K. Our results show that the crystal structure of stoichiometric $Pb_3Mn_7O_{15}$ has a pronounced 2-dimensional character and can be described in the orthorhombic space group *Pnma*.

1. Introduction

Since the discovery of the colossal magneto-resistance (CMR) effect in (La, Pb)MnO_3 [2], manganites have been comprehensively investigated throughout the last years [3]. Extensive studies focused especially on members of two groups: the perovskite-type compounds (space groups $R\bar{3}m$, *Pnma*) and the layered compounds of the so-called Ruddlesden–Popper series (space group $I/4mmm$) with the general formula $A_{n+1}Mn_nO_{3n+1}$, where *A* is a rare-earth metal and *n* is the number of corner-shared MnO_6 octahedral sheets forming the layer [3,4].

$Pb_3Mn_7O_{15}$ cannot be classified in either of these groups, although, like the $n=1$ compounds of the Ruddlesden–Popper series, it grows in a pronounced crystalline anisotropy with alternating monolayers of MnO_6 octahedra and PbO sheets. The first synthesis was reported in literature already 30 years ago [5], but until recent times little was known about the physical properties. No evidence of CMR is present in the pure compound. Nevertheless, the layered type structure and the presence of a mixed valence state of Mn ions (Mn^{3+}/Mn^{4+}) recently motivated a new thorough investigation: Magnetization and specific heat measurements on $Pb_3Mn_7O_{15}$ revealed several magnetic phases including long-range magnetic ordering below $T_N = 70$ K [1] and paramagnetic charge localization at $T_{CL} = 250$ K. Dielectric properties give rise to formation of polarons, which make $Pb_3Mn_7O_{15}$ a promising candidate for multiferroic materials [6].

However, the basis for further microscopic investigations of the physical properties is the exact knowledge of the crystal symmetry. The structural properties of the layered compound $Pb_3Mn_7O_{15}$ have been a matter of debate since the first report on its structure by Darriet et al. [5], using single crystal X-ray diffraction data taken with a laboratory K_α molybdenum source. The crystallographic structure was refined based on the orthorhombic space group $Cmc2_1$. Marsh and Herbstein [7] reformulated the structure based on the data of Darriet et al. [5] in the orthorhombic space group *Cmcm* which involved shifting the origin by about 0.25 in *z*-direction. Symmetrizing the positions of some pairs of atoms by shifts up to 0.2 Å was thereby necessary. Shortly afterwards, Le Page and Calvert [8] found that a description

* Corresponding author at: Institut Laue-Langevin, 6 rue Jules Horowitz, BP 156, 38042 Grenoble Cedex 9, France. Fax: +33 476207688.
E-mail address: rasch@ill.fr (J.C.E. Rasch).

0022-4596/$ - see front matter © 2009 Elsevier Inc. All rights reserved.
doi:10.1016/j.jssc.2009.02.001

in $P6_3/mcm$ discloses a new class of systematic absences not accounted for previously. The new hexagonal unit cell of $Pb_3Mn_7O_{15}$ is related to the orthorhombic description in *Cmcm* by $\mathbf{a}_{hex} = (\mathbf{a}_{ortho} - \mathbf{b}_{ortho})/2$, $\mathbf{b}_{hex} = \mathbf{b}_{ortho}$, $\mathbf{c}_{hex} = \mathbf{c}_{ortho}$. Nevertheless, Weissenberg and Laue patterns also indicate contradictory results concerning hexagonal and orthorhombic symmetry [5]. In order to settle this discrepancy between the different models and in order to investigate the structural properties as a function of temperature, we performed new measurements on this material employing high-resolution synchrotron radiation.

2. Experimental details

2.1. Sample preparation and characterization

Single crystals were grown by the flux method, as described in [1]. The flux agent PbO was chosen since it is known as an effective solvent for many oxide compounds and allows to avoid incorporation of foreign ions into the lattice. The synthesis of $Pb_3Mn_7O_{15}$ single crystals started with heating a mixture of 93% by weight of high purity PbO and 7% by weight of Mn_2O_3 in a platinum crucible at 1000 °C for 4 h. Afterwards, the crucible was cooled to 900 °C at a cooling rate of 2.5 °C/h, followed by non-constrained cooling to room temperature. Single crystals with a plate-like hexagonal form and a shiny black surface were found on the solidified liquid surface. The plates measured up to 40 mm in diameter and were extracted mechanically from the flux. Afterwards, the crystals were carefully ground for synchrotron powder diffraction investigations.

Thermogravimetric analysis was employed to verify the oxygen content in our sample. The powder sample was heated from room temperature up to 800 °C in a 5% H_2/95% He flux at a heating rate of 2 °C/min. A mass spectrometer analyzed the evolution of H_2O. Finally, from the weight loss of the sample the initial oxygen content was calculated. The oxygen content of our sample has been determined to $Pb_3Mn_7O_x$ with $x = 14.93 \pm 0.05$.

2.2. High-resolution synchrotron measurements

High-resolution synchrotron radiation powder diffraction patterns were collected at the powder diffraction station of the Swiss Light Source Materials Science (SLS-MS) beamline using a multicrystal analyzer detector [9,10]. The instrumental contribution to the peak profile was reduced to negligible levels by carefully optimizing the beamline optics and the detector while observing the crystal analyzer rocking curve with the attenuated direct beam [11]. The photon energy ($\lambda = 0.617793(1)$ Å) was determined using the silicon standard from NIST Si640c, whereas the instrumental resolution function was evaluated using $Na_2Ca_3Al_2F_{14}$, a standard powder known for being characterized by Bragg peaks with a negligible intrinsic contribution to the instrumental line shape. During the acquisitions, the detector arm was continuously rotated at a constant speed, recording the data at high reading frequency, which are rebinned to the appropriate step size after the measurements. Temperature dependent measurements between 15 and 295 K in steps of 50 K were performed using the Janis Cryostat. The $Pb_3Mn_7O_{15}$ powder was mounted in the cryostat in 0.2 mm Lindemann capillaries and the capillary spun at approximately 10 Hz during the 2θ scan to avoid preferred orientation. The collected data were refined using the program Fullprof [12] based on Rietveld refinement.

3. Results

The powder diffraction pattern at $T = 15$ K is shown in Fig. 1.

Refinements, based on hexagonal space group $P6_3/mcm$ reported earlier [8], gave unsatisfactory agreement with the observed pattern, due to a systematic splitting of peaks indicating a lowering of the space group symmetry. Orthorhombic $Cmc2_1$ [5] and *Cmcm* [7] describe the major peak splitting well but mismatch a large number of small peaks in the pattern at high angles 2θ. The inset of Fig. 1 shows a small angular section around the expected (110) reflection in a hexagonal setting as reported by Le Page and Calvert [8]. The splitting was observed at all temperatures, excluding a structural phase transition as shown by the continuous change of the orthogonal distortion, not reaching the hexagonal symmetry up to 295 K. The value of splitting shows a temperature dependence and amounts to $2\theta = 0.03^\circ$ at $T = 295$ K to $2\theta = 0.1^\circ$ at $T = 15$ K. From an investigation of the subgroup relationships starting from the high symmetry hexagonal $P6_3/mcm$ structure, the orthorhombic space group *Pnma* is obtained. The different structures reported earlier are related in the following way: orthorhombic *Cmcm* used by Marsh and Herbstein [7] is a *translationsgleiche* subgroup (a symmetry element is removed, but translation symmetry is maintained) of $P6_3/mcm$ of index 3. $Cmc2_1$ used by Darriet et al. [5] is also *translationsgleich* of index 2 of space group *Cmcm*. Space group *Pnma* is reached by a *klassengleiche* subgroup (in our case, the C-centering has been removed) of *Cmcm* of index 2. The crystallographic *a*-axis is now perpendicular to the layers, in contrast to previous descriptions with perpendicular *c*-axis.

All preceding interpretations were based on the same data set taken by Darriet et al. [5] on a laboratory X-ray single crystal diffractometer. Although the angular resolution at the synchrotron is considerably improved compared to a laboratory instrument, the peak splitting of about $2\theta = 0.03^\circ$ at room temperature is resolvable on a standard X-ray laboratory instrument. A possible explanation for the discrepancy in the structural description might be a different oxygen content of our sample compared to the previous studies. Investigations on the layered manganites $BaTb_2Mn_2O_7$ and $BaSm_2Mn_2O_7$ [13,14] have shown that phase transitions from tetragonal to orthorhombic symmetry occur as a function of oxygen or nitrogen annealing, suggesting some tolerance for oxygen non-stoichiometry.

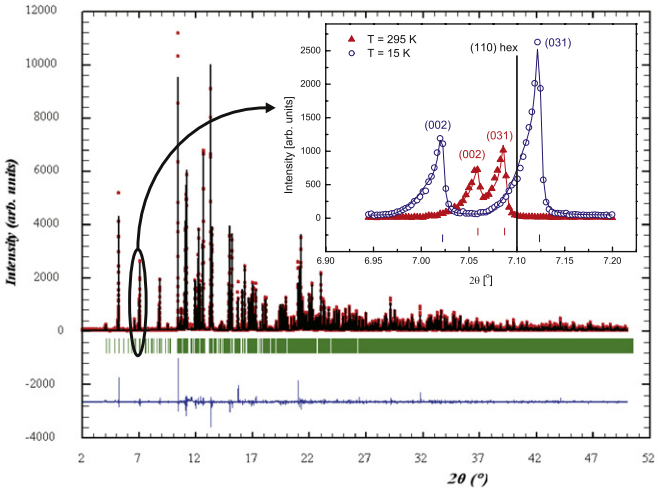

Fig. 1. Observed and calculated X-ray synchrotron powder diffraction pattern of $Pb_3Mn_7O_{15}$ at $T = 15$ K. The inset shows the splitting of the hexagonal (110) reflection into orthorhombic (002) and (031) at $T = 15$ K (open circles, blue online) and $T = 295$ K (closed triangles, red online). Please note the interchange of the hexagonal *c*-axis with the orthorhombic *a*-axis. (For interpretation of the references to color in this figure legend, the reader is referred to the web version of this article.)

Table 1
Comparison of structural models of $Pb_3Mn_7O_{15}$.

Reference	[5]	[7]	[8]	This paper	This paper
Temperature (K)	295	295	295	295	15
Space group	$Cmc2_1$ (No. 36) orthorhombic	$Cmcm$ (No. 63) orthorhombic	$P6_3/mcm$ (No. 193) hexagonal	$Pnma$ (No. 62) orthorhombic	$Pnma$ (No. 62) orthorhombic
Cell parameters					
a (Å)	17.28 (1)	17.28 (1)	9.98 (1)	13.59510 (2)	13.55128 (2)
b (Å)	9.98 (1)	9.98 (1)	9.98 (1)	17.29544 (3)	17.14898 (2)
c (Å)	13.55 (1)	13.55 (1)	13.55 (1)	10.03813 (1)	10.0909 (1)
Volume (Å^3)	2336.76	2336.76	1168.78	2360.30	2345.03
Data	[5]	[5]	[5]	SLS-MS	SLS-MS
Sample	Single crystal			Polycrystalline	Polycrystalline
Wavelength (Å)	Mo $K\alpha$			0.617793 (1)	0.617793 (1)
Number of reflections	904			n.a.	n.a.
$\sin(\Theta/\lambda)$ (Å^{-1})	0.67			0.65	0.65
χ^2				1.70	2.26
R (%)				13.8	8.9
R_{Bragg} [%]				6.9	4.4

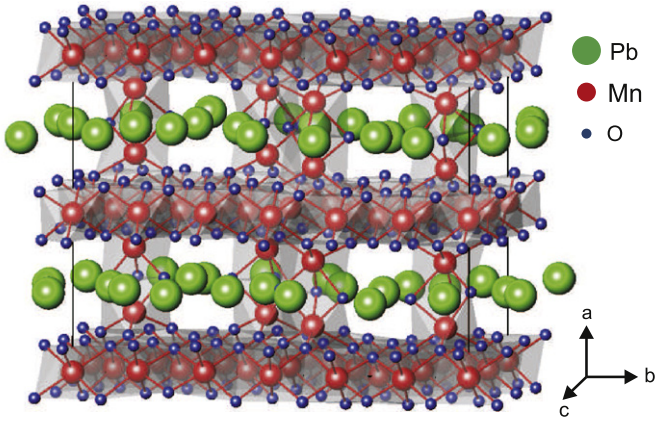

Fig. 2. Layered structure of $Pb_3Mn_7O_{15}$. The Pb atoms are interconnecting the Mn–O-layers (on-line version: Mn (red); O (blue); Pb (green)). (For interpretation of the references to color in this figure legend, the reader is referred to the web version of this article.)

Based on the *Pnma* space group we obtained satisfactory agreement between the measured data sets and calculations ($R = 8.9\%$ for $T = 15$ K and $R = 13.8\%$ for $T = 295$ K) as shown in Table 1. The unit cell comprises eight formula units leading to 30 independent atoms per unit cell (see Fig. 2). The atomic positions at $T = 295$ and 15 K are listed in Tables 2 and 3, respectively. Manganese ions are distributed among the general 8*d* position and the special positions 4*a*, 4*b* and 4*c*. The MnO_6 octahedra can be grouped into undistorted (4*a*, 4*b*), weakly distorted (4*c*, 8*d*), and strongly distorted octahedra (8*d*) with respect to the angles of the main axis of the octahedra (see Table 4). The weakly and undistorted octahedra form layers around $x = 0$ and 0.5 bridged by pairs of strongly distorted octahedra. The decrease in temperature goes with a reduction of the lattice constant b with simultaneous increase along the c direction, so that the pseudo-hexagonal arrangement of Mn atoms gets stretched along c at low temperatures. The variation of lattice parameters as function of temperature is shown in Fig 3.

As reported earlier [5], the Pb atoms, equally located on two different symmetry sites 8*d* and 4*c*, are closely confined around layers at $x = 0.25$ and 0.75, half-way in-between the MnO_6 layers. Projected on the (100) planes the lead atoms lie on lines along the ⟨011⟩ and ⟨001⟩ directions. At $T = 15$ K the lead atoms get displaced as indicated in Fig. 4, where the atoms of the $x = 0.25$ layers are systematically shifted towards the positive c directions, while atoms on the $x = 0.75$ layer are shifted in the opposite direction. The

Table 2
Refined parameters for $Pb_3Mn_7O_{15}$ at $T = 295$ K.

Atom	Type	Site	x	y	z	B_{iso} (Å^2)
Pb1	Pb	8*d*	0.2492 (2)	0.4439 (1)	0.4395 (2)	0.97 (1)
Pb2	Pb	8*d*	0.2574 (2)	0.1186 (1)	0.1107 (2)	0.97 (1)
Pb3	Pb	4*c*	0.7711 (2)	0.25	0.9897 (3)	0.97 (1)
Pb4	Pb	4*c*	0.7596 (2)	0.25	0.6452 (2)	0.97 (1)
Mn1	Mn	8*d*	0.0047 (7)	0.0814 (4)	0.245 (1)	0.86 (4)
Mn2	Mn	8*d*	0.0091 (5)	0.3340 (5)	0.499 (1)	0.86 (4)
Mn3	Mn	8*d*	0.5104 (5)	0.1652 (5)	0.509 (1)	0.86 (4)
Mn4	Mn	8*d*	0.1513 (6)	0.4174 (5)	0.742 (1)	0.86 (4)
Mn5	Mn	8*d*	0.3566 (5)	0.0832 (5)	0.748 (1)	0.86 (4)
Mn6	Mn	4*a*	0	0	0	0.86 (4)
Mn7	Mn	4*b*	0	0	0.5	0.86 (4)
Mn8	Mn	4*c*	0.5073 (9)	0.25	0.258 (2)	0.86 (4)
Mn9	Mn	4*c*	0.5115 (9)	0.25	0.758 (2)	0.86 (4)
O1	O	8*d*	0.085 (2)	0.497 (2)	0.339 (4)	1.2 (1)
O2	O	8*d*	0.420 (2)	0.008 (2)	0.342 (4)	1.2 (1)
O3	O	8*d*	0.262 (2)	0.506 (1)	0.155 (3)	1.2 (1)
O4	O	8*d*	0.932 (2)	0.326 (2)	0.656 (3)	1.2 (1)
O5	O	8*d*	0.597 (2)	0.172 (2)	0.670 (4)	1.2 (1)
O6	O	4*c*	0.939 (3)	0.25	0.420 (5)	1.2 (1)
O7	O	4*c*	0.580 (3)	0.25	0.417 (5)	1.2 (1)
O8	O	4*c*	0.435 (3)	0.25	0.596 (5)	1.2 (1)
O9	O	4*c*	0.090 (3)	0.25	0.566 (5)	1.2 (1)
O10	O	8*d*	0.910 (3)	0.588 (2)	0.424 (4)	1.2 (1)
O11	O	8*d*	0.581 (3)	0.922 (2)	0.421 (4)	1.2 (1)
O12	O	8*d*	0.078 (2)	0.332 (2)	0.334 (4)	1.2 (1)
O13	O	8*d*	0.427 (2)	0.164 (2)	0.334 (4)	1.2 (1)
O14	O	8*d*	0.231 (2)	0.666 (2)	0.181 (3)	1.2 (1)
O15	O	8*d*	0.236 (3)	0.926 (1)	0.394 (3)	1.2 (1)
O16	O	8*d*	0.928 (3)	0.412 (2)	0.415 (4)	1.2 (1)
O17	O	8*d*	0.580 (3)	0.086 (2)	0.427 (4)	1.2 (1)

Data have been collected at the Swiss Light Source Materials Science (SLS-MS) beamline with a wavelength $\lambda = 0.617793(1)$ Å, $\sin(\theta_{max}/\lambda) = 0.649$ Å^{-1}. Refinement has been performed in the orthorhombic space group *Pnma* (No. 62), $Z = 8$.

observed changes of lattice parameters and lattice displacements with cooling show that the *Pnma* structure is more stable than the former hexagonal description for temperatures below room temperature. We remind that the previously reported hexagonal axis is in our description along a, i.e. perpendicular to the $b-c$ plane.

4. Discussion

As discussed by Volkov et al. [1] there are two factors which can cause polyhedral distortions of the MnO_6 octahedra in

Table 3
Refined parameters for $Pb_3Mn_7O_{15}$ at $T = 15$ K.

Atom	Type	Site	x	y	z	B_{iso} (Å^2)
Pb1	Pb	8*d*	0.2481 (1)	0.44475 (6)	0.4346 (1)	0.028 (6)
Pb2	Pb	8*d*	0.2556 (1)	0.11965 (6)	0.10753 (9)	0.028 (6)
Pb3	Pb	4*c*	0.7716 (1)	0.25	0.9908 (2)	0.028 (6)
Pb4	Pb	4*c*	0.7544 (2)	0.25	0.6500 (1)	0.028 (6)
Mn1	Mn	8*d*	0.0018 (5)	0.0818 (2)	0.2429 (7)	0.17 (3)
Mn2	Mn	8*d*	0.0067 (3)	0.3345 (3)	0.4982 (6)	0.17 (3)
Mn3	Mn	8*d*	0.5081 (3)	0.1659 (3)	0.5117 (6)	0.17 (3)
Mn4	Mn	8*d*	0.1515 (4)	0.4167 (4)	0.7411 (6)	0.17 (3)
Mn5	Mn	8*d*	0.3570 (4)	0.0823 (4)	0.7426 (6)	0.17 (3)
Mn6	Mn	4*a*	0	0	0	0.17 (3)
Mn7	Mn	4*b*	0	0	0.5	0.17 (3)
Mn8	Mn	4*c*	0.5013 (7)	0.25	0.246 (1)	0.17 (3)
Mn9	Mn	4*c*	0.5128 (6)	0.25	0.7625 (9)	0.17 (3)
O1	O	8*d*	0.083 (2)	0.500 (1)	0.326 (3)	0.14 (8)
O2	O	8*d*	0.418 (2)	0.011 (1)	0.342 (2)	0.14 (8)
O3	O	8*d*	0.261 (2)	0.5096 (9)	0.150 (2)	0.14 (8)
O4	O	8*d*	0.931 (1)	0.325 (1)	0.658 (2)	0.14 (8)
O5	O	8*d*	0.597 (1)	0.171 (1)	0.686 (2)	0.14 (8)
O6	O	4*c*	0.929 (2)	0.25	0.410 (3)	0.14 (8)
O7	O	4*c*	0.574 (2)	0.25	0.429 (3)	0.14 (8)
O8	O	4*c*	0.445 (2)	0.25	0.582 (3)	0.14 (8)
O9	O	4*c*	0.083 (2)	0.25	0.584 (3)	0.14 (8)
O10	O	8*d*	0.912 (2)	0.585 (1)	0.434 (2)	0.14 (8)
O11	O	8*d*	0.580 (2)	0.920 (1)	0.416 (2)	0.14 (8)
O12	O	8*d*	0.079 (1)	0.330 (1)	0.336 (2)	0.14 (8)
O13	O	8*d*	0.427 (1)	0.167 (1)	0.314 (2)	0.14(8)
O14	O	8*d*	0.235 (2)	0.6645 (9)	0.178 (2)	0.14 (8)
O15	O	8*d*	0.243 (2)	0.9228 (9)	0.386 (2)	0.14 (8)
O16	O	8*d*	0.929 (2)	0.422 (1)	0.433 (2)	0.14 (8)
O17	O	8*d*	0.579 (2)	0.088 (1)	0.419 (2)	0.14 (8)

Data have been collected at the Swiss Light Source Materials Science (SLS-MS) beamline with a wavelength $\lambda = 0.617793(1)$ Å, $\sin(\theta_{max}/\lambda) = 0.649$ Å^{-1}. Refinement has been performed in the orthorhombic space group *Pnma* (No. 62), $Z = 8$.

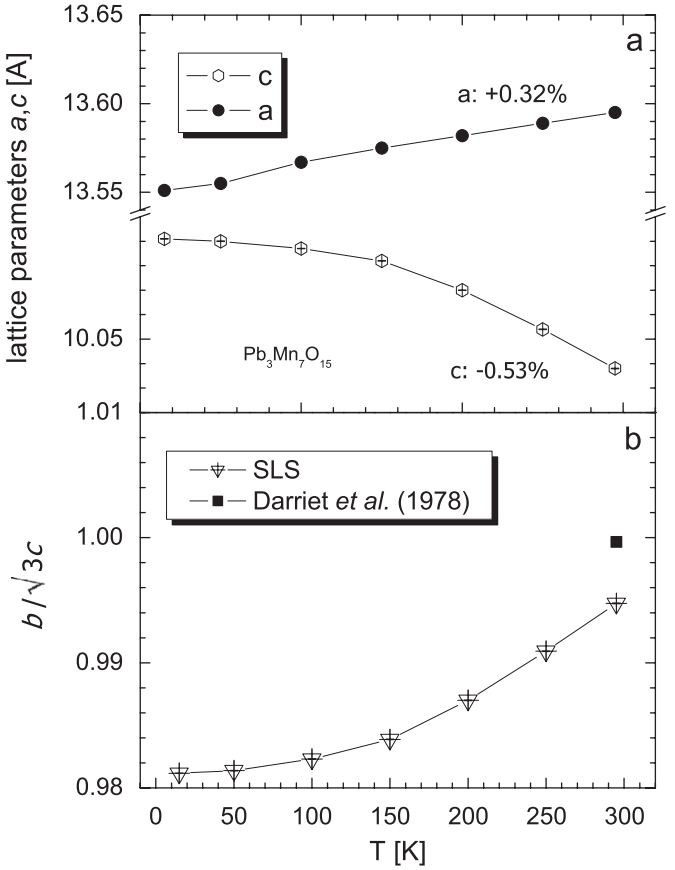

Fig. 3. (a) Temperature dependence of the lattice parameters a and c in $Pb_3Mn_7O_{15}$. The orthogonal a-axis is vertical to the layer structure and corresponds to the hexagonal c-axis in the description of [8]. (b) The in-plane lattice parameter ratio corresponding to the hexagonal lattice (black square) is not reached up to 295 K, therefore only an orthorhombic description (open triangles) is possible in our case.

Table 4
O–Mn–O angles α and atomic distances d(O−Mn), d(Mn−O) of the MnO_6 octahedra in $Pb_3Mn_7O_{15}$ at $T = 15$ K.

Atom	Site		α	d(O−Mn)	d(Mn−O)	BVS
Mn1	8*d*	O1–Mn1–O12	172 (2)	1.97 (2)	1.86 (2)	+3.46 (9)
		O2–Mn1–O12	173 (2)	1.87 (2)	2.06 (2)	
		O16–Mn1–O17	174 (2)	2.16 (2)	1.94 (2)	
Mn2	8*d*	O4–Mn2–O12	173 (2)	1.92 (2)	1.91 (2)	+3.70 (9)
		O6–Mn2–O10	174 (2)	2.00 (2)	1.89 (2)	
		O9–Mn2–O16	174 (2)	1.98 (2)	1.95 (2)	
Mn3	8*d*	O5–Mn3–O13	174 (2)	2.14 (2)	2.28 (2)	+3.33 (8)
		O7–Mn3–O11	172 (2)	1.89 (2)	2.04 (2)	
		O8–Mn3–O17	172 (2)	1.82 (2)	1.89 (2)	
Mn4	8d	O2–Mn4–O14	160 (2)	2.13 (2)	2.17 (2)	+3.12 (8)
		O3–Mn4–O5	164 (2)	1.96 (2)	1.84 (2)	
		O10–Mn4–O15	162 (2)	1.97 (2)	2.05 (2)	
Mn5	8*d*	O1–Mn5–O14	167 (2)	1.83 (2)	2.00 (2)	+3.42 (9)
		O3–Mn5–O4	162 (2)	2.24 (2)	2.13 (2)	
		O11–Mn5–O15	165 (2)	1.81 (2)	1.98 (2)	
Mn6	4*a*	O2–Mn6–O2	180 (2)	1.95 (2)	1.95 (2)	+3.39 (8)
		O11–Mn6–O11	180 (2)	1.94 (2)	1.94 (2)	
		O17–Mn6–O17	180 (2)	2.03 (2)	2.03 (2)	
Mn7	4*b*	O1–Mn7–O1	180 (2)	2.08 (3)	2.08 (3)	+3.8 (1)
		O10–Mn7–O10	180 (2)	2.00 (2)	2.00 (2)	
		O16–Mn7–O16	180 (2)	1.77 (2)	1.77 (2)	
Mn8	4*c*	O6–Mn8–O7	176 (3)	1.85 (3)	2.09 (3)	+3.9 (1)
		O12–Mn8–O13	175 (2)	1.92 (2)	1.88 (2)	
		O6–Mn8–O7	175 (2)	1.92 (2)	1.88 (2)	
Mn9	4*c*	O4–Mn9–O5	178 (2)	1.88 (2)	1.93 (2)	+4.0 (1)
		O4–Mn9–O5	178 (2)	1.88 (2)	1.93 (2)	
		O8–Mn9–O9	175 (3)	2.04 (3)	1.82 (3)	

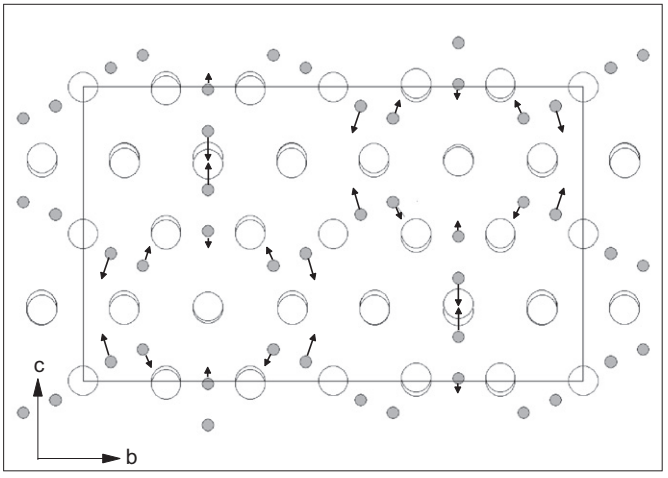

Fig. 4. Projection of the low temperature structure ($T = 15$ K) on the b–c plane. Only manganese (white open circles) and lead (gray closed circles) are shown. Arrows indicate the direction of displacements of the lead atoms from $T = 295$ to 15 K.

$Pb_3Mn_7O_{15}$. The first factor is the Jahn–Teller effect which originates from degenerate orbital states of the Mn^{3+} ions in a regular octahedral crystal field. The valence state of the Mn ions is discussed explicitly below. Secondly the stereo-active lone pairs of the $6s^2$ electrons in Pb^{2+} can lead to significant shifts of some oxygen positions due to repulsion of the lone pair with Pb–O

bonds. This assumption can be supported by the fact, that strongly distorted MnO_6 octahedra consist of oxygen ions which are in close proximity to Pb ions.

According to the stoichiometry of the formula unit, the Mn ions in $Pb_3Mn_7O_{15}$ are in a mixed valence state Mn^{3+}/Mn^{4+} with a ratio 4/3. Assuming the Jahn–Teller effect to be responsible for the distortion, one can distribute Mn^{3+} ions onto interlayer Mn sites (Mn4, Mn5) and Mn^{4+} ions onto the undistorted positions (Mn6, Mn7) in a straightforward way. Assuming further that the remaining Mn atoms have equal probability to be in either of the oxidation state, one obtains the total ratio of $Mn^{3+}/Mn^{4+} = 4/3$ corresponding to the stoichiometry of the formula unit. The distribution of tri- and tetravalent Mn ions can be estimated from Mn–O bond lengths via bond-valence sums (BVS). The BVS is proportional to the sum over the deviation $(r_0 - r)$, where r is the measured bond length and r_0 an empirical parameter for the mean cation–anion distance. Since the r_0 values for Mn^{3+} and Mn^{4+} are very similar, one single r_0 value (1.76 Å) can be used as an estimate for the calculations [15]. The result (Table 4) is less satisfactory than reported by Volkov et al. [1], but we assume it more accurate since the lower symmetric space group we used allows an investigation of non-averaged bond-lengths. After this analysis it is less evident to connect unambiguously the strongly distorted octahedra (Mn4, Mn5) with the Jahn–Teller effect (see Table 4). At this point no final conclusion can be drawn about the mixed valence state in $Pb_3Mn_7O_{15}$ since Mn ions on all crystallographic sites seem to be in average in a state between tri- and tetravalency which cannot be connected to the degree of octahedral distortion.

5. Conclusions

We re-investigated the mixed valence Mn^{3+}/Mn^{4+} manganite $Pb_3Mn_7O_{14.93}$ using X-ray synchrotron powder diffraction. In contrast to Darriet et al. [5] the oxygen content was verified by thermogravimetry. This is essential as oxygen is released in the growth process above 840 °C. Rietveld refinement showed that our data can be well described within the orthorhombic space group *Pnma* and that there is no structural phase transition in the observed temperature range $15 \leqslant T \leqslant 295$ K. The refined space group is different to several previous descriptions reported in literature, which were all analyzed from the data set taken by Darriet et al. [5]. The crystal symmetry stays unchanged in the investigated temperature regime, the pseudo-hexagonal arrangement of the Mn atoms gets stretched along the *c*-axis at low temperatures and the Pb atoms experience a systematic displacement. Earlier investigations [1] based on a higher symmetry phase and magnetization data suggest three different types of MnO_6 octahedra distinguished by the degree of distortion and the valence state of the Mn ions. Our synchrotron measurements on the same crystals as in [1] show that this classification is less significant in the lower symmetric description and that BVS calculations could not clarify unambiguously the Mn valence states.

Acknowledgments

Synchrotron beam time at the Swiss Light Source Materials Science beamline Powder Diffraction Station is gratefully acknowledged as well as the support of the crystal growth department of the L.V. Kirensky Institute in Krasnoyarsk and the Laboratory for Developments and Methods (LDM) of the PSI. The work is supported by INTAS Grant 06-1000013-9002 of the Russian Academy of Science (RAS), Siberian Branch.

References

[1] N.V. Volkov, K.A. Sablina, O.A. Bayukov, E.V. Eremin, G.A. Petrakovskii, D.A. Velikanov, A.D. Balaev, A.F. Bovina, P. Boni, E. Clementyev, J. Phys. Condens. Matter 20 (2008) 055217.
[2] C.W. Searle, S.T. Wang, Can. J. Phys. 47 (1969) 2703.
[3] see e.g. T. Chatterji, Colossal Magnetoresistance Manganites, Kluwer Academic, Dordrecht, 2004.
[4] Y. Tokura, Colossal Magnetoresistive Oxides, Advances in Condensed Matter Science, vol. 2, Gordon and Breach Science Publisher, London, 2000.
[5] P.B. Darriet, M. Devalette, B. Latourrette, Acta Cryst. B 34 (1978) 3528.
[6] N.V. Volkov, K.A. Sablina, E.V. Eremin, P. Boni, Sh. Valloppilly, I.N. Flerov, A. Kartashev, J.C.E. Rasch, M. Boehm, J. Schefer, J. Phys. Condens. Matter 20 (2008) 445217.
[7] R.E. Marsh, F.H. Herbstein, Acta Cryst. B 39 (1983) 280.
[8] Y. Le Page, L.D. Calvert, Acta Cryst. C 40 (1984) 1787.
[9] J.-L. Hodeau, P. Bordet, M. Anne, A. Prat, A.N. Fitch, E. Dooryhee, G. Vaughan, A.K. Freund, in: Proceedings of the SPIE, vol. 3448, 1998, p. 353.
[10] F. Gozzo, B. Schmitt, Th. Bortolamedi, C. Giannini, A. Guagliardi, M. Lange, D. Meister, D. Maden, P. Willmott, B.D. Patterson, J. Alloys Compd. 362 (2004) 206.
[11] F. Gozzo, L. De Caro, C. Giannini, A. Guagliardi, B. Schmitt, A. Prodi, J. Appl. Cryst. 39 (2007) 347.
[12] J. Rodriguez-Carvajal, FullProf: a program for Rietveld refinement and pattern matching analysis, Abstracts of the Satellite Meeting on Powder Diffraction of the XV Congress of the IUCr, Toulouse, France, 1990, p. 127.
[13] N. Kamegashira, S. Umeno, Mater. Chem. Phys. 16 (1987) 89.
[14] N. Kamegashira, S. Umeno, Jpn. J. Appl. Phys. 25 (1986) L238.
[15] I.D. Brown, D. Altermatt, Acta Cryst. B 41 (1985) 244.